RICE UNIVERSITY

Coupling of Nanoparticle and Metallodielectric Grating Plasmons

By

Jeremy M. Dumoit

A THESIS SUBMITTED
IN PARTIAL FULFILLMENT OF THE
REQUIREMENTS FOR THE DEGREE

Master of Science

APPROVED, THESIS COMMITTEE:

Naomi J. Halas, Director,
Stanley C. Moore Professor of Electrical and
Computer Engineering,
Professor of Chemistry

Jason H. Hafner, Chair,
Assistant Professor of Physics & Astronomy,
Assistant Professor of Chemistry

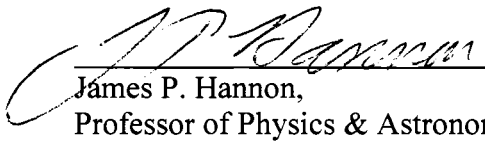

James P. Hannon,
Professor of Physics & Astronomy,

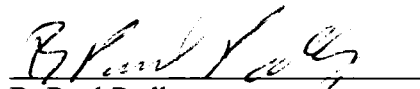

B. Paul Padley,
Professor of Physics & Astronomy,
Assistant Professor of Chemistry

HOUSTON, TEXAS
DECEMBER 2006

Abstract

Coupling of Nanoparticle and Metallodielectric Grating Plasmons

by

Jeremy M. Dumoit

Coupled plasmonic systems have been in the limelight recently for both their interesting fundamental physical properties, and their possible applications in sensing and opto-electrical system integration. Planar plasmonic systems, which can couple propagating and localized plasmons, show promise for integration of future on-chip optoelectronic devices. This thesis investigates such a system consisting of a planar metallodielectric grating coupled to spherical gold nanoparticles. It is shown that the addition of gold nanoparticles to a silver metallodielectric grating system can produce a profound change in the resonance response of the system. This coupling is shown to depend strongly on the size and surface coverage density of the gold nanoparticles.

Acknowledgments

My education at Rice has been a learning experience in every sense. I've thoroughly enjoyed the courses I have taken and have also enjoyed learning some very exciting and beautiful physics. My sincere thanks are extended to Nate Grady, Britt Lassiter and Carly Levin for many interesting discussions. Thank you to Camille Keefe for being so understanding about my unorthodox schedule and my many all-nighters. Additionally, my thanks are extended to Jun Kono for teaching physics in an inspiring way. Finally, I would like to thank Dr. Naomi Halas for the opportunity to learn so much about academia, research, and, most importantly, myself.

Table of Contents

List of Figures

Chapter 1

Introduction

It seems that many new advances in technology utilizing plasmonics are on the horizon. The ability to detect substances of extremely minute concentration, a possible cure for some cancers, a possible method for integrating current microchips with light, and even an invisibility cloak are just a few of the developments that are being studied using plasmonic structures. With ideas as exciting as these, it's no wonder that the field of plasmonics is receiving so much attention lately.

The existence of plasmons, however, is not a new discovery. The physicist Robert W. Wood first discovered plasmonic effects via optical measurements on gratings in 1902 at Johns Hopkins University[1]. Though Wood didn't realize what he was seeing; and hence the term 'Wood's Anomaly'; he was the first to note the presence of plasmons in an optical spectrum.

A localized surface plasmon is the collective oscillation of the conduction band electrons of a metal, occurring at the interface between the metal and a dielectric material. The resonant frequency of the surface plasmon of a structure is dependent on the dielectric of the metal and the surrounding dielectric environment, as well as the geometry and size of the nanostructure itself. There has been a deluge of novel

nanostructures and fabrication techniques reported over the past decade[2, 3, and 4]. Some shapes and their respective plasmons resonances are shown below (figure 1.1).

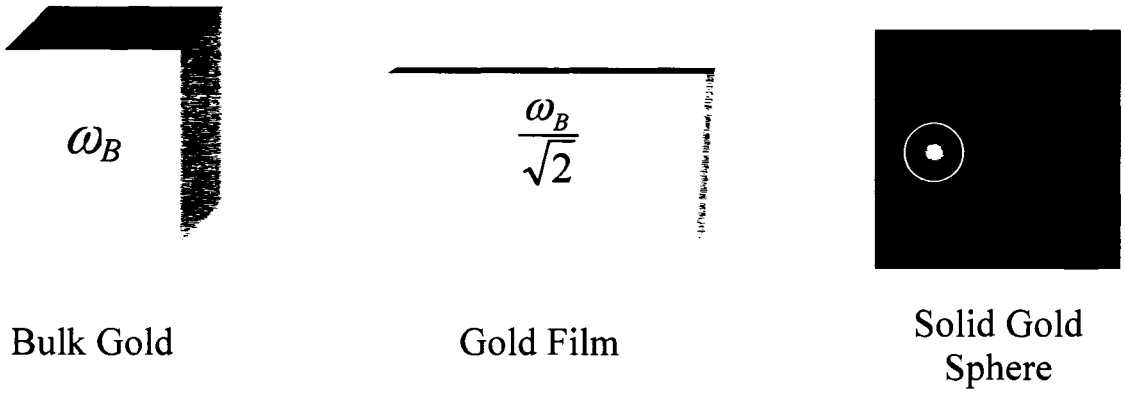

Figure 1.1 - Plasmon frequencies for some common solid nanostructures including bulk gold, a thin gold film, and colloidal gold particles.

There is a new family of composite nanoparticles of which one can 'tune' the plasmon resonance frequency without changing the overall size of the particle. One such structure is the gold nanoshell[5]. A nanoshell consists of a spherical silica core surrounded by a concentric thin gold shell (See figure 1.2). The radius of the core is denoted as R_1, and the radius of the entire structure, including shell, is given by R_2. Thus the shell thickness is given by $R_2 - R_1$. The plasmon resonance frequency is dependent on the ratio of R_1 and R_2. By adjusting this ratio in the fabrication process, the particles can be tuned without changing their overall size.

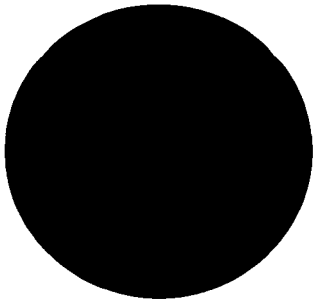

$$\omega_{sp} = \frac{\omega_B^2}{2} \cdot \left(1 \pm \frac{\sqrt{1 + 8\left(\frac{R_1}{R_2}\right)^3}}{3} \right)$$

Figure 1.2 – Gold nanoshell with silica core of radius R_1 encapsulated by gold shell of thickness $R_2 - R_1$. As shown, the plasmon resonance depends on the ratio of R_1 to R_2.

The above expression for the plasmon resonance of a nanoshell was derived using a semi-classical model assuming an incompressible fluid of electrons. Traditionally, Mie scattering theory is used to calculate the response of spherical particles. Mie theory utilizes and expansion of the electric potential I terms of the spherical Bessel function basis. However, Mie scattering theory is limited to spherical geometries. Plasmon hybridization, an analogue to molecular orbital theory is a more general method to analyze complex plasmonic nanostructures[6]. This theory describes the nanoshell plasmon as a hybridization of a metal sphere plasmon and a hollow metallic cavity plasmon (See figure 1.3). The primitive sphere and cavity plasmons hybridize in two modes: a low-energy mode where the dipoles of both the sphere and cavity point in the same direction (bonding), and a higher energy mode, where the sphere and cavity dipoles are pointing in opposite directions (anti-bonding). For spherical systems, plasmon hybridization provides an alternative to Mie scattering theory, while providing more insight into the physics of the plasmon. Plasmon hybridization is also a useful way for

describing coupled nanosystems such as particles over a film[7] and particles coupled with a metal nanowire[8].

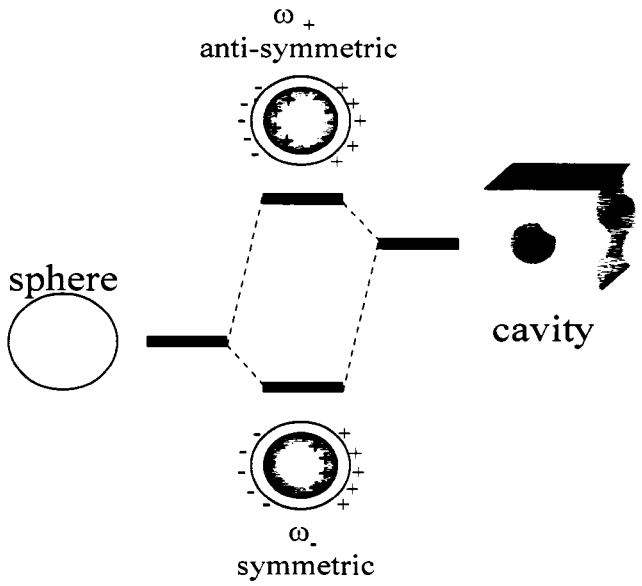

Figure 1.3 – Plasmon hybridization model for a nanoshell. The light and dark (bonding and anti-bonding) nanoshell plasmon modes are a hybridization of metallic sphere and cavity plasmons.

Another structure that has a plasmon response, and is the focus of this research, is a metallodielectric grating[9, 10, 11]. This grating structure consists of metal strips uniformly spaced with a sub-wavelength period on a planar dielectric substrate (See figure 1.4). Metallodielectric gratings are unique plasmonic structures because they allow light to be coupled into the plasmon modes directly without using a prism. Traditionally, a surface plasmon on a metallic film has to be excited using a prism, as in the Kretschmann geometry (See figure 1.5).

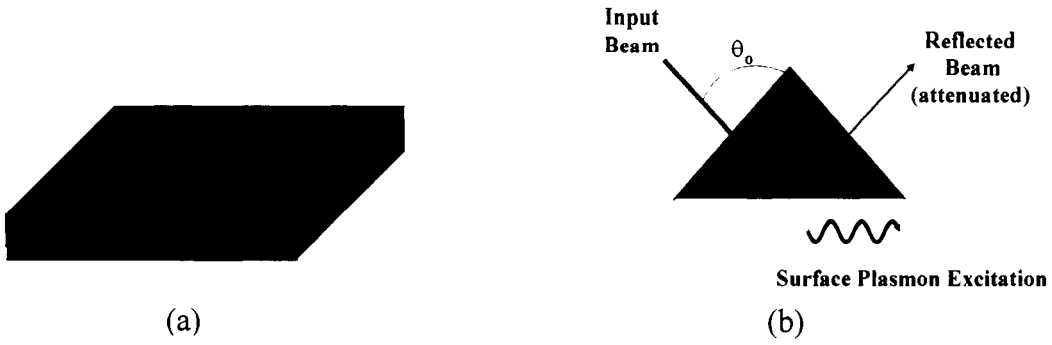

(a) (b)

Figure 1.4 – (a) Metallodielectric grating system consists of silver strips periodically arranged on a dielectric substrate with a sub-wavelength period. (b) Kretschmann geometry. A metal film is deposited directly onto a prism. The prism couples light into the film plasmon via total internal reflection.

The momentum of the incident light is given by: $\frac{\hbar\omega}{c}$. This is normally less than the momentum of the surface plasmon, and thus prevents incident light from coupling directly to the surface plasmon mode. However, the prism provides the extra momentum dependent on its dielectric and angle of incidence: $\sqrt{\varepsilon}\frac{\hbar\omega}{c}\cdot\sin\theta_0$ [11]. The metallodielectric grating system, like the Kretschmann geometry as described above, is able to provide the extra momentum needed to couple incident light directly into the surface plasmon mode by the following mechanism: For a grating with a period of a, the grating vector is defined as follows: $g=\frac{2\pi}{a}$. The dispersion relation for a planer film surface plasmon is written as: $k_x=\frac{\omega}{c}\sin\theta$, where k_x is a wave vector component along the film surface. The metallodielectric grating adds momentum in integral chunks of the grating vector. The dispersion relation thus becomes: $k_x=\frac{\omega}{c}\sin\theta\pm n\vec{g}$, where n is an

integer.

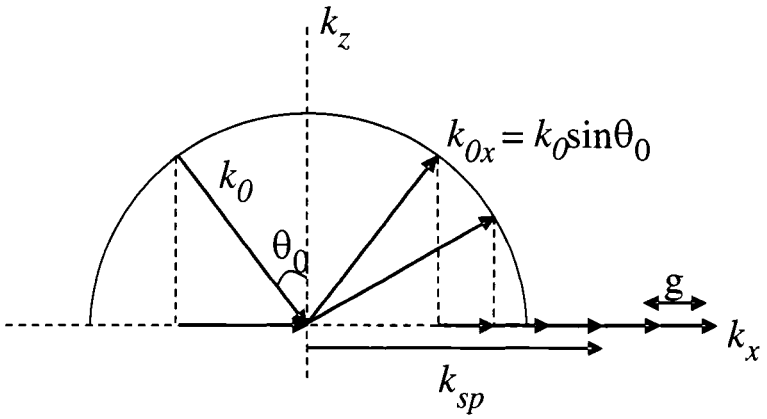

Figure 1.5 – Extra momentum is provided by the grating in integer multiples of the grating vector. This give the projection of the wave vector onto the surface enough momentum to couple directly to the surface plasmon mode.

The dispersion relation is a useful way to think about surface plasmons and how light couples to the plasmon modes. In figure 1.6 below, the grating provides the momentum needed to couple the incident light to the surface plasmon mode. (Figure 1.6)

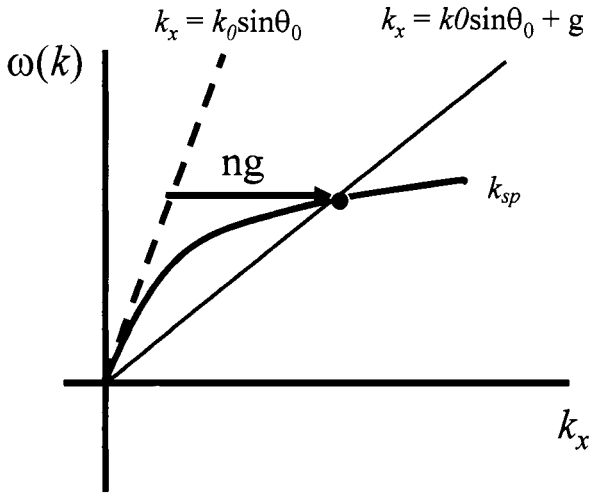

Figure 1.6 – Dispersion diagram for a grating system. The incident light line is shown in blue. The surface plasmon is excited when the light momentum line intersects the surface plasmon line. This extra momentum, again, is provided by the grating.

Unlike a film plasmon, grating plasmons support two modes separated by a frequency gap at the zone boundary[12]. The two modes are the standing wave solutions for the grating systems and correspond to the charge distributions in the metallic strips as shown in figure 1.7.

(a) (b)

Figure 1.7 – The two allowed plasmon modes for a rectangular profile grating: (a) low energy anti-symmetric standing wave plasmon mode and (b) higher energy symmetric plasmon mode.

For gratings with a sinusoidal surface profile containing only one Fourier component, the plasmon can be excited up to the light line, but not beyond. However, for gratings with a surface profile which contains higher order periodic components, the plasmon modes may be excited beyond the zone boundaries all the way to normal incidence. While the relative phase of the surface profile components has no effect on the size of the energy gap, it may have a profound effect on the coupling of the modes around normal incidence. [7] Below is a typical plot of the plasmon dispersion for a grating system of multiple surface profile components. Note that, as mentioned above, the behavior around k=0 (normal incidence) is strongly dependent on the surface profile of the grating

and the relative phase of its components.

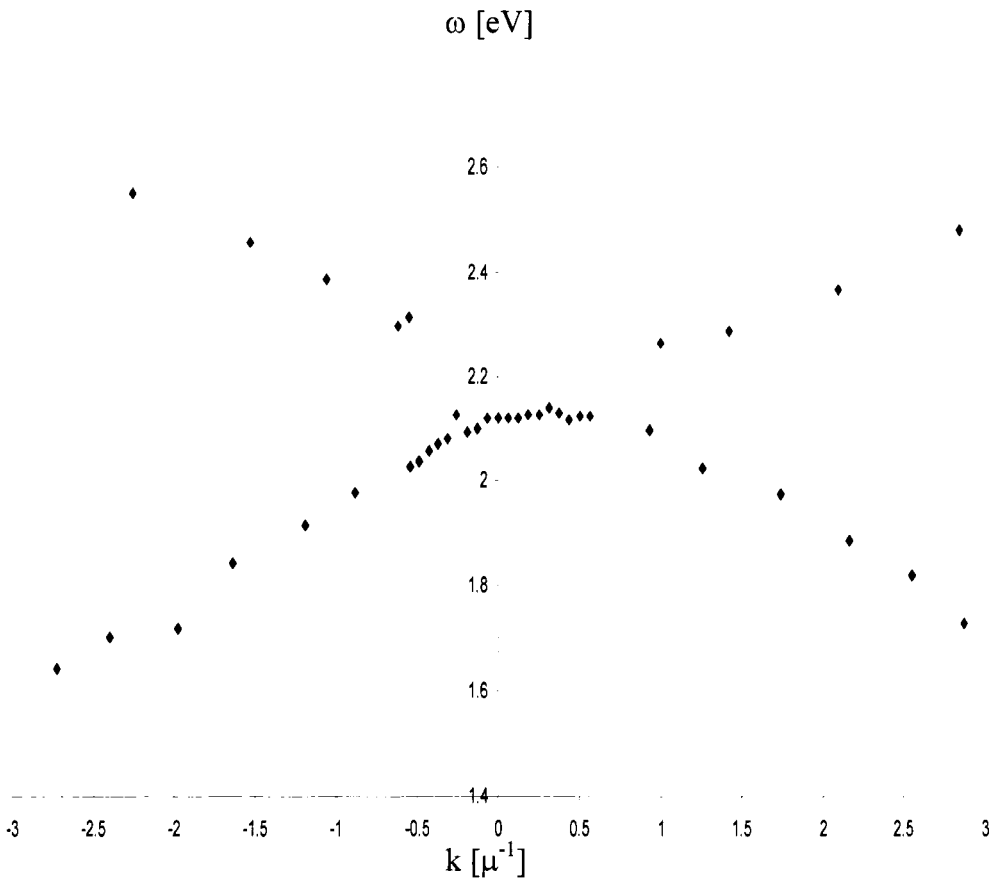

Figure 1.8 – Typical dispersion curve for metallodielectric grating: ω in eV versus *k* in inverse microns. The two plasmon modes are evidenced by the two branches with an energy gap near normal incidence.

Chapter 2

Metallodielectric Grating Fabrication

Planer plasmonic nanostructures promise to bridge the gap between optical and electronic devices. Reproducible and scaleable fabrication procedures will be required before any such devices are feasible for mainstream use. Microcontact printing has been used to fabricate periodic nanostructures in the past, and is used here to pattern the metallodielectric gratings[10, 13, 14]. The microcontact printing method involves fabricating a PDMS stamp using a commercial diffraction grating as a template. The PDMS stamp is used to apply a metal-adhesive ink grating pattern onto a glass slide. This ink pattern can then be preferentially plated with metal such that a ruled metal grating is formed on the glass slide that is the plasmonic structure of interest in this text. The details of this procedure follow:

First, a PDMS (poly-dimethyl siloxane) stamp is made from a commercially available holographic brazed diffraction grating. The template gratings were obtained from Edumnd Optics and have a period of 555 nm. Using a quick-drying multi-purpose epoxy, the stamps were glued to standard glass microscope slides to make them easier to

handle. The PDMS is prepared by combining the polymer and curing agent in a 10:1 mass ratio and mixing well. Approximately 20 grams of PDMS are required per stamp. The PDMS and curing agent are mixed by hand for approximately 5 minutes and then poured into the vessel used to hold the stamp for curing; in this case 30 ml poly-ethylene Petri dishes.

Compared to the features being fabricated, any air bubbles introduced into the PDMS from mixing are macroscopic. Therefore the PDMS is degassed by placing the Petri dishes in the access chamber of a glove box and slowly pumping down the chamber to avoid the PDMS boiling over. After degassing the PDMS, the template stamp is placed face down into the PDMS. The glass slide rests against the sides of the dish, creating a space of ~2-3 mm between the surface of the diffraction grating and the bottom of the dish (See figure 2.1).

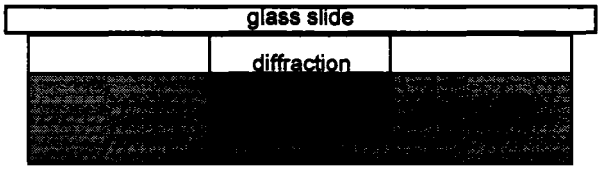

Figure 2.1 – PDMS stamp fabrication: diffraction grating glued to glass slide, resting in petri dish with 2 mm gap.

Different curing methods were tried. The best results occurred when the PDMS was allowed to cure overnight at room temperature. Two hours in an oven at 70 C also cured the polymer; however it was not always possible to successfully remove the

template grating from the cured PDMS after baking. After curing, the template grating was removed from the PDMS and the stamp was cut into fourths, being careful to mark on the bottom the direction of the grating vector. Each of these fourths will be referred to as a PDMS stamp in this text.

The dielectric substrate used in this research is a glass microscope slide. The stamping process is as follows: (i) the slide was cut into ~1cm x 1cm squares and cleaned with piranha (H_2SO_4 and H_2O_2 in 7:3 ratio) for 30 minutes. (ii) PTMS (poly-trimethyl siloxane) ink is then prepared by adding 1-2 drops of PTMS to 10 ml of 200 proof EtOH. (iii) PDMS stamps are then 'inked' by submerging the patterned surface of the stamp in the PTMS solution. The inked stamps are allowed to dry for approximately 15 minutes; until any PTMS droplets have visibly evaporated from the stamp surface. (iv) the stamp is gently 'rolled' onto the glass slide starting with one edge and lightly pressing toward the opposite edge. (v) the PTMS is allowed to cure at room temperature for 24 hours before the stamps are removed.

Metallizing the PTMS grating pattern is accomplished using an electroless silver plating method[9, 10, 14]. The plating solution used in fabrication was obtained from Peacock Chemical and consists of four components. Components A, B, and C are diluted with milli-q water in a ratio of 1:29 by volume. The #93 activator solution is diluted with milli-q water in by adding 6 ml water to 200 μl #93. The metallization process is as follows: (i) the slide surface is first activated by applying enough #93 to cover the surface, and removing the excess with the pipette. (ii) slides are affixed to a plastic circle via AFM sample stickers, and this circle is then stuck to the bottom of a plastic dipping basket with tape. Between 4 and 8 slides are typically metallized at once. (iii) dilute

solutions A, B and C are mixed and the basket is submerged in the mixture for 10 – 20 seconds. (iv) the basket is immediately submerged in milli-q water upon removal to quench the metallization process. (v) the back of each slide is swabbed with EtOH to remove any unwanted silver. (vi) slides are finally dried with nitrogen.

This success of this process has been found to be highly dependent on the quality of diffraction grating used initially, metallization time, and pressure used in the stamping of the slides. The template diffraction gratings may be utilized to fabricate two sets of PDMS stamps at most before being replaced. Likewise, the metallization solution ages quickly and older solutions require shorter plating times, and tend to produce overgrown gratings with a continuous silver layer. The PDMS stamps themselves may be reused multiple times before requiring cleaning – which can be accomplished in an ultrasonic acetone bath.

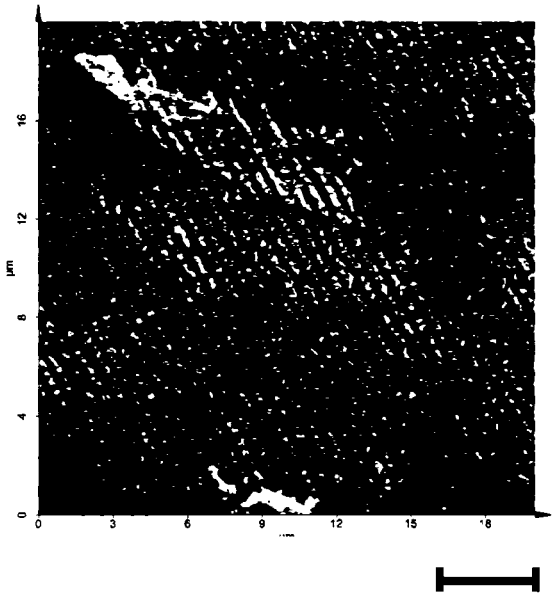

Figure 2.2 - AFM image of a 555 nm period Ag grating fabricated using the process described. Scale bar is 3 microns.

After grating fabrication, gold nanoparticles are drop-dry deposited on the Ag metallodielectric gratings. The grating surface is first coated with PVP (poly-vinyl pyrrodine). To make the PVP solution, solid PVP is dissolved in EtOH to yield a 0.1% by mass solution of PVP (.008 g PVP for 10 ml of EtOH). 300 μl of this solution is spin coated at 2500 rmp for 30 seconds on the grating. This produces a 3 – 5 nm layer of PVP on the grating surface [11]. The desired size of Au colloid is then drop deposited on the grating. The surface coverage is dependent on deposition time. Deposition times ranging from 30 min to 2 hours were used here. The gold colloid used was purchased from Ted Pella and manufactured by British Biocell International.

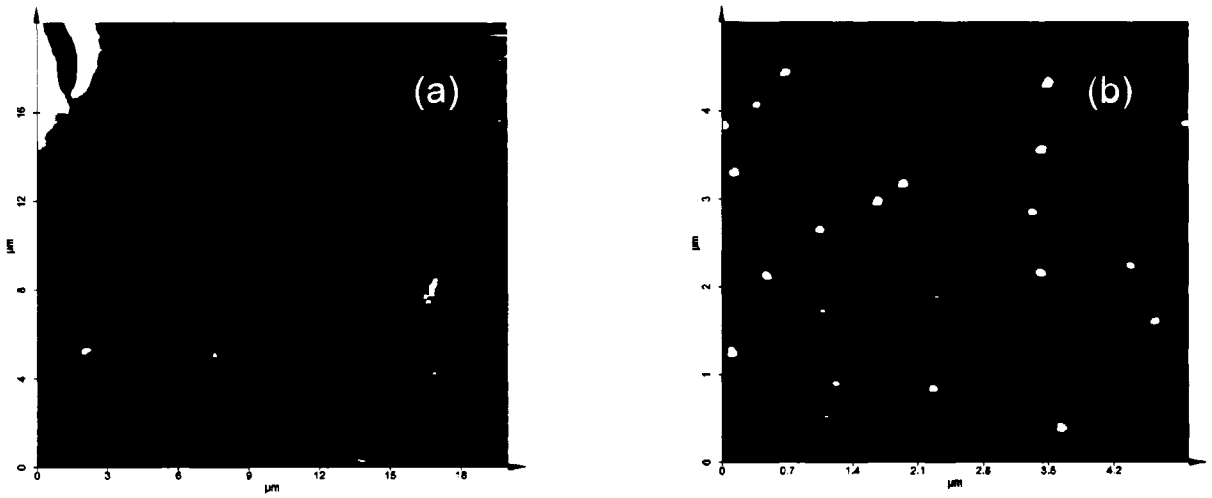

Figure 2.3 - AFM images of a 555 nm period Ag grating with 50 nm Au colloid deposited in the method described above. (a) Expanded view showing average surface coverage and (b) a zoomed in view showing that ~ 75% of the colloid is situated on top of the metal strips rather than in the gaps.

Remaining colloid solution is washed from the grating surface gently with milli-q water and, finally, the grating is dried with nitrogen.

Chapter 3

Effects of Au Colloid Coupling on Grating Plasmon Dispersion

This project was started with the goal of spanning a large parameter space of grating periods and colloid sizes to identify the regime which produces strong plasmon coupling. However, interesting results early on, and difficulty in sample fabrication narrowed the focus to gratings of period 555 nm exclusively.

To probe the plasmonic response of the metallodielectric grating systems variable angle transmission spectroscopy was used. The samples were affixed to a rotational stage in a Varian Cary 5000 UV-Vis spectrometer. A Glan-Taylor polarizer, which covered the entire wavelength range of interest, was placed between the beam and the sample to create an s-polarized incident beam. For a fixed angle of incidence, a transmission spectrum over a range of wavelengths from 400 nm to 1100 nm was collected. By varying the angle of incidence between -19 degrees and +19 degrees from normal, we were able to identify the plasmon resonances as a function of varying k_x, and thus produce the plasmon dispersion diagrams.

Shown below (Fig 3.1) are transmission spectra for five angles of a 555 nm Ag grating on glass, fabricated and spin-coated with PVP using the methods described in chapter two. A transmission spectrum of a plain glass slide at normal incidence was used

as a background. The resonances of the two plasmon modes of the metallodielectric grating are clearly visible in the 500 – 700 nm wavelength range.

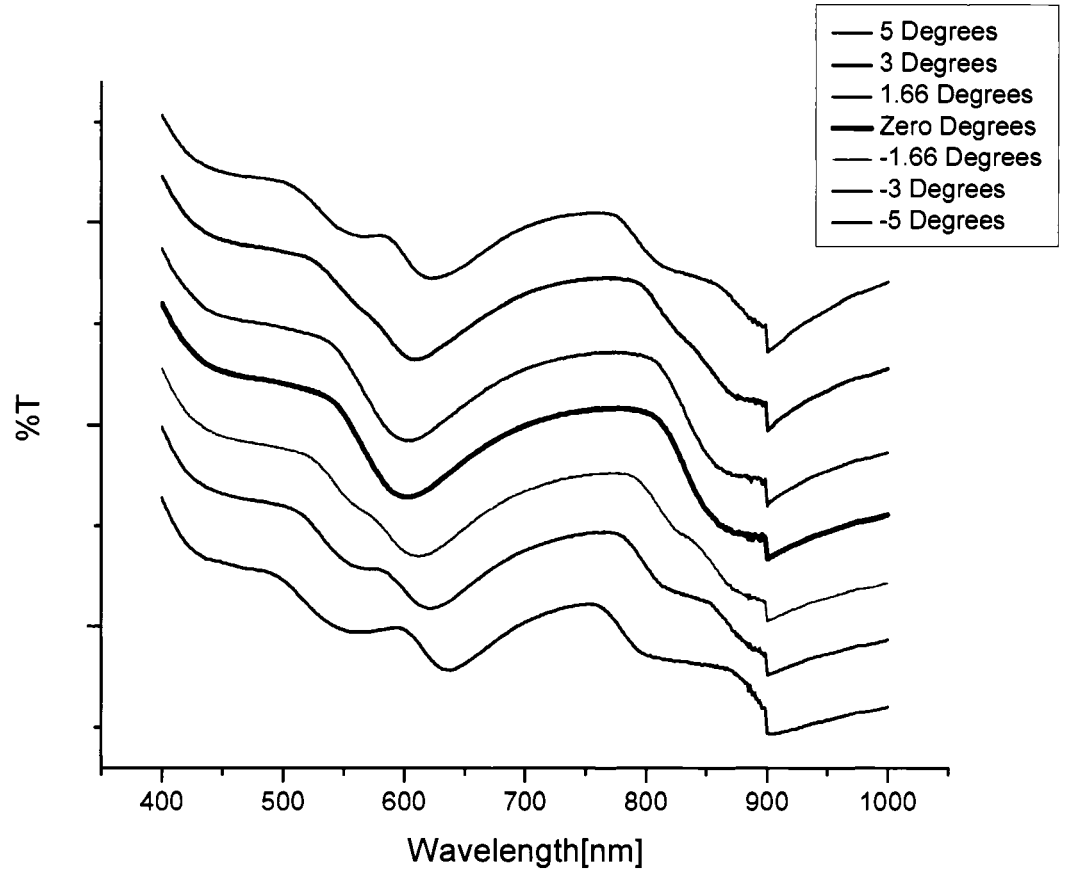

Figure 3.1 – (Color) – Transmission spectra at seven different angles of incidence on a 555 nm period Ag grating on glass spin coated with 0.1% PVP solution. The excitation of the plasmon modes is clearly evident as a dip in the transmission.

The resonances of the two standing wave grating plasmon modes are identified by the dips in the transmission between 500 and 700 nm wavelength.

The dispersion relations (ω vs. k) are plotted using the spectra to identify the plasmon resonance for each wave vector. Following is a dispersion diagram for the same 555 nm period Ag grating coated with PVP as measured above in the spectra (Fig 3.1).

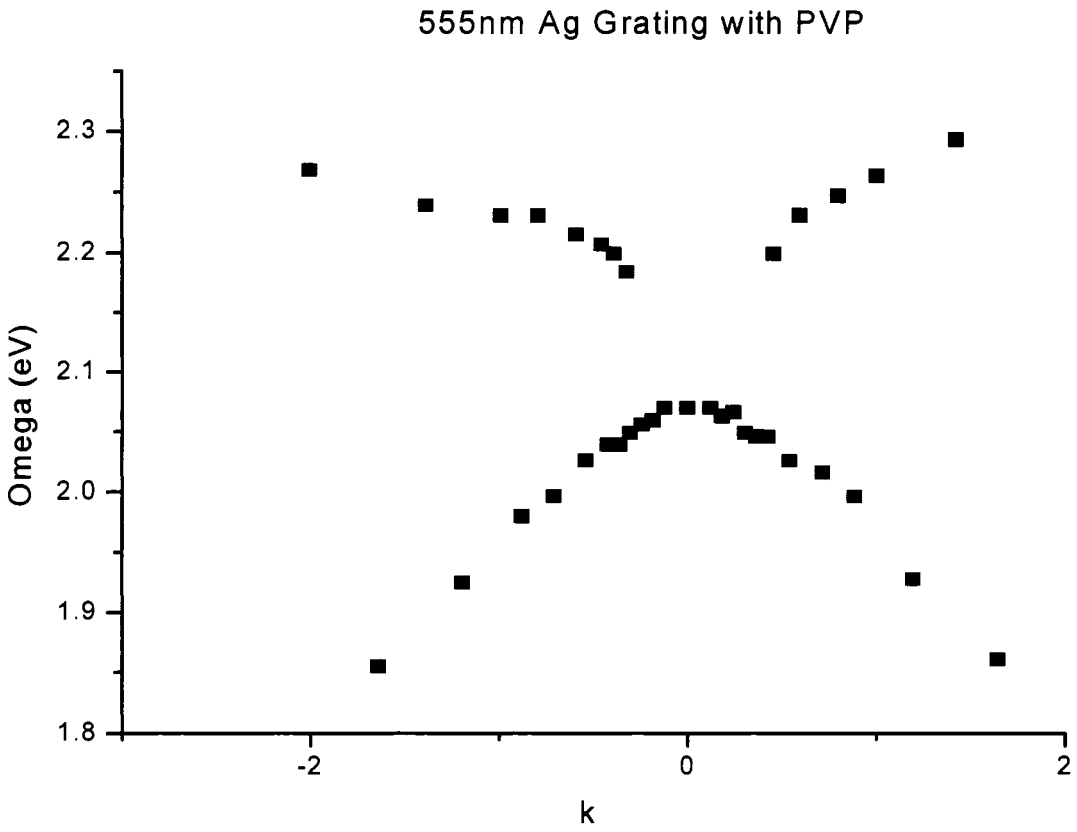

Figure 3.2 – (Color) – The dispersion relation deduced from the spectra of the 555 nm period Ag grating shown in Figure 3.1.

Figure 3.2, above, is a typical dispersion relation for a metallodielectric grating. Though not surprising[12, 15], it should be noted that a plasmon mode is excited at normal incidence. As mentioned in the introduction, the dispersion behavior near the normal incidence is strongly dependent on the surface profile of the grating. The fabrication method used here produces a strip profile that is near rectangular. Such a shape must contain a large number of higher-order Fourier components. These higher order components allow coupling even at normal incidence[12]. Another observation is that only one plasmon mode is visible at normal incidence. This has been observed previously for

these types of metallodielectric grating structures[10, 14] and is probably due to interference effects cause by the surface profile components of the grating[12].

The plasmon dispersion of the plain, PVP-coated 555 nm metallodielectric grating was compared to systems where either 50 nm or 100 nm Au colloid was then deposited onto the same grating. Below, the dispersion relations for the plain gratings coated with PVP are plotted together with the dispersion relations of the same grating with Au colloid deposited on the surface (Figures 3.3 and 3.4).

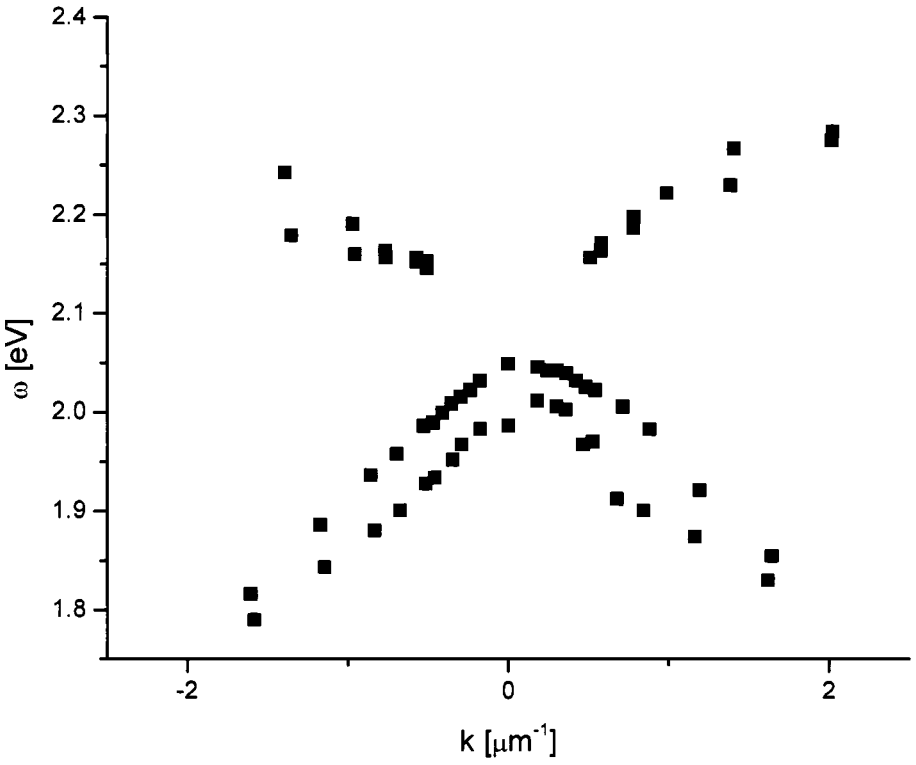

Figure 3.3 – (Color) – Dispersion plot of a 555 nm metallodielectric grating on glass without 50 nm diameter Au colloid (Blue) compared to the same grating with 50 nm Au colloid (Red).

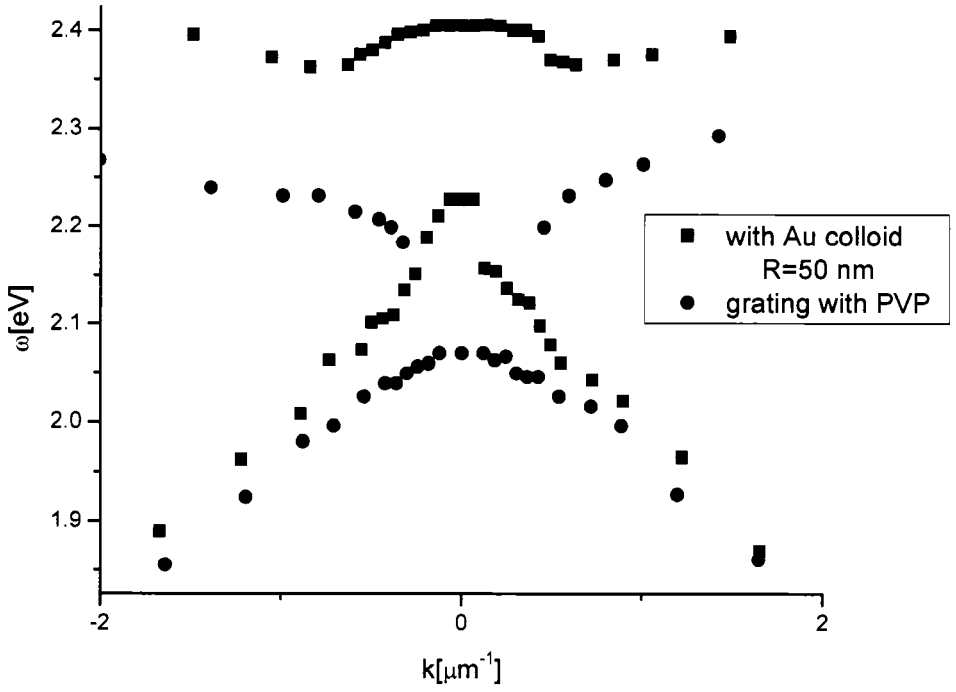

Figure 3.4 – (Color) – Dispersion relation of 555 nm grating with just PVP (Green) compared to the same grating with 100 nm Au colloid.

The grating-colloid systems probed in figures 3.3 and 3.4 differ only in size of the nanoparticles deposited. The fabrication methods, deposition time and data acquisition methods were the same. While the 50 nm colloid appears to have no profound effect on the dispersion of the grating plasmons, the 100 nm produces a dramatic change. Perhaps the most evident difference is the excitation of both plasmon modes at normal incidence. The energy of each plasmon mode is shifted higher by ~ 12% at normal incidence with the addition of the 100 nm Au colloid.

This result was found to be highly dependent on particle coverage. When the deposition time was reduced from the original one hour, to only 30 minutes, the strong

coupling previously seen for the 100 nm Au colloid disappeared. However, when repeating a third time, with a deposition time of one hour, the coupling response was again strong.

Chapter 4

Conclusions

A non-trivial effect is caused by the addition of gold nanoparticles in the vicinity of the metallodielectric grating. This effect is highly dependent on particle size and surface coverage. There are a few possibilities of what could be causing this coupling effect. First, how might the particles be altering the overall geometry of the grating itself? The 555 nm period Ag gratings we have fabricated consist of metal strips approximately 30 nm tall and 445 nm wide. Thus the gaps between metal strips are ~ 110 nm across. Depending on the particle size, and where it is situated on the grating, the particles may effectively make the metal strips wider, or short out the metal strips by bridging the gap between adjacent one. (See figure 4.1).

Another possibility is that most of the particles are sitting on top of the metal strips, thereby increasing the effective thickness of the strips greatly in some areas. Since the diameter of the colloid used was 1.7 to 3.3 times the thickness of the grating strips, the increase in thickness imparted by colloid deposited on top of the strips is substantial. The same is true for colloid in the gaps; while the grating period remains unchanged (unless the gap is shorted), the ratio of metal strip to space is increased.

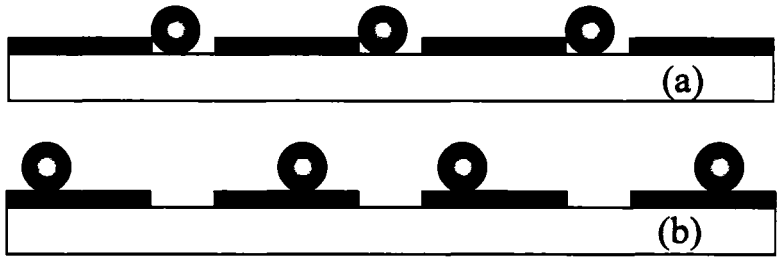

Figure 4.1 – (Color) – (a) Au colloid show sitting in the gaps between metal strips of the grating. The period would remain unchanged, but the width of the strips would be increased by the diameter of the particle. (b) Au colloid resting on top of the strips. The effective thickness of the strips is almost tripled or more.

A Matlab simulation based on the Lochbihler method[10, 16] was used to examine the effects of widening the metal strips, while keeping the grating period constant. This results in an overall red-shift of both plasmon modes, but does not lead to an avoided crossing near normal incidence, as seen in the data. The effect of increasing the thickness of the grating strips has already been reported[12], and can result in both plasmon modes being visible at normal incidence. The authors refer to this as 'over-coupling' of light, and report two dips in reflectance, separated by a plateau, at normal incidence. This corresponds well to the two dips in transmission as seen in our data. It should be noted, however, that the gratings they are examining have a sinusoidal profile with a 2nd harmonic element; rather than a rectangular profile. This conclusion may be supported by the observation that ~ 75% of the colloid deposited are sitting on top of the metal strips, as visible in the AFM images (Fig. 2.3).

A final possibility is that this change in dispersion behavior is due to the hybridization between the grating and particle plasmons, much like that which has been

reported for a spherical particle over a film[7]. In a particle over a film system, at certain frequencies, the particle and film plasmons interact, thereby creating a hybridized virtual state. The strength of this coupling is completely dependent on the ratio of particle diameter to film thickness. Staying within an order of magnitude size difference, the higher this ratio is, the stronger the coupling effect. The thickness of the grating strips is analogous to the film thickness in the grating system, and thus, the larger the particle diameter, the stronger the particle grating hybridization we would expect. This is consistent with the results obtained here, and suggests the presence of a hybridized state similar to that in the film-particle system.

Future directions for this research include more in-depth SEM particle coverage versus coupling strength studies. Further theoretical modeling of different geometries is also needed to understand how particle position affects the plasmonic response of the system.

Bibliography

[1] Wood, R. W. Anomalous Diffraction Gratings. *Physical Review* 48, 928-936 (1935).

[2] Cuncheng Li, Weiping Cai,* Yue Li, Jinlian Hu, and Peisheng Liu. Ultrasonically Induced Au Nanoprisms, and their Size Manipulation Base on Aging. *J. Phys. Chem. B* 110:1546 – 1552, 2006.

[3] Min Hu, Hristina Petrova, Jingyi Chen, Joseph M. McLellan, Andrew R. Siekkinen, Manuel Marquez, Xingde Li, Younan Xia, and Gregory V. Hartland, Ultrafast Laser Studies of the Photothermal Properties of Gold Nanocages, *J. Phys. Chem.,* 110 (4), 1520 -1524, 2006

[4] Kang Yeol Lee, Minjung Kim, Joeoong Hahn, Jung Sang Suh, Inhyung Lee, Kwan Kim, and Sang Woo Han, Assembly of Metal Nanoparticle-Carbon Nanotube Composite Materials at the Liquid/Liquid Interface, *Langmuir,* 22 (4), 1817 -1821, 2006

[5] S. Oldenburg, R. D. Averitt, S. Westcott, and N. J. Halas, Nanoengineering of Optical Resonances, *Chem. Phys. Lett.* 288, 243 (1998).

[6] E. Prodan, C. Radloff, N. J. Halas, and P. Nordlander. A hybridization model for the plasmon response of complex nanostructures. *Science*, 302:419–422, 2003.

[7] P. Nordlander, and E. Prodan. Plasmon Hybridization in Nanoparticles near Metallic Surfaces. *Nano Lett.*, 4:2209-2213, 2004

[8] F. Hao, and P. Nordlander. Plasmonic coupling between a metallic nanosphere and a thin metallic wire. *Appl. Phys. Lett.* 89, 103101 (2006)

[9] Moran, C. E., Steele, J. M. & Halas, N. J. Chemical and dielectric manipulation of the plasmonic band gap of metallodielectric arrays. *submitted* (2004).

[10] Steele, J. M., Moran, C.E., Lee, A., Aguirre, C.M. & Halas, N.J. Metallodielectric gratings with subwavelength slots: Optical properties. *Physical Review B* 68, 205103 (2003).

[11] Raether, H. R. *Surface Plasmons on Smooth and Rough Surfaces and on Gratings* (Springer-Verlag, New York, 1988).

[12] Barnes, W. L., Preist, T. W., Kitson, S. C. & Sambles, J. R. Physical origin of photonic energy gaps in the propagation of surface plasmons on gratings. *Physical Review B* 54, 6227-6244 (1996).

[13] Moran, C. E., Radloff, C. & Halas, N. J. Benchtop fabrication of submicrometer metal line and island Arrays using passivative microcontact printing and electroless plating. *Advanced Materials* 15, 804-+ (2003).

[14] Sri Priya Sundararajan, Jennifer M. Steele, Naomi J. Halas. Propagation of surface plasmons on Ag and Cu extended one-dimensional arrays on silicon substrates, *Applied Physics Letters* 88, 063115 (2006).

[15] Porto, J. A., Garcia-Vidal, F. J. & Pendry, J. B. Transmission resonances on metallic gratings with very narrow slits. *Physical Review Letters* 83, 2845-2848 (1999).

[16] Lochbihler, H. & Depine, R. A. Characterization of highly conducting wire gratings using an electromagnetic theory of diffraction. *Optics Communications* 1000, 231-239 (1993).